Organic Process Research & Development **2001**, *5*, 299−307

Optimization and Control of Dynamic Bioprocesses

D. L. Stoner,*,† A. P. Poloski, J. A. Johnson, and C. R. Tolle
Biotechnology Department, Idaho National Engineering and Environmental Laboratory, P.O. Box 1625, 2525 Fremont Avenue, Idaho Falls, Idaho 83415-2203

Abstract:

For many applications, such as commodity chemical production, ore leaching, waste treatment, and environmental remediation, bioprocesses can be less expensive, more energy-efficient, and more environmentally friendly than conventional processes. The key to effective implementation of bioprocesses is rational design, optimization, and process control. We are applying the tools of intelligent systems to develop supervisory systems for the optimization and control of continuous, dynamic, and uncharacterized bioprocesses. We have designed, built, and evaluated hierarchical hardware and software systems for the control of microbial oxidation of soluble iron in a continuous stirred tank reactor. The supervisory control module uses stochastic learning to determine what system parameters (i.e., pH, dilution rate, and temperature) should be, based on the state of the system. An expert-based flow-rate controller optimizes reactor performance for each set of system parameters. Theoretically, high reactor conversion can be obtained much faster by varying these multiple parameters simultaneously as opposed to the traditional method of varying a single parameter at any given instance.

1. Introduction

Operating a reactor such that the yield of a specific product is at a maximal level has been an important topic in chemical engineering. Typically, a model of the system is formulated around the reaction kinetics and type of reactor. From this point, an optimization problem can usually be solved and the optimal operating conditions determined. These optimal parameters are used as set points for the reactor control system. However, for biological systems, the reaction kinetics of a new process involving a new substance or reactant cannot usually be obtained unless a comprehensive laboratory analysis has been carried out, which may take considerable time to complete.

Development of control systems that do not depend on comprehensive laboratory analyses yet reach optimal reactor performance have been the focus of much research. Most of the research on control systems has been done in support of the food, pharmaceutical, and specialty-chemical industries. These industries typically involve batch processes controlled by expert systems or fuzzy expert systems. An example of this control methodology applied to a batch bioprocesses involves the work of Halme et al.[1] and Hitzmann et al.[2] Their work incorporates the accumulated experience of plant operators to determine the proper time course for batch fermentation. Some applications have been found for neural-network and fuzzy-logic systems. Kishimoto et al.[3] have used a fuzzy-logic control system for the glucose feed rate in the production of glutamic acid. Oishi et al.[4] simulated temperature control in the sake brewing process using fuzzy logic. Optimization-based techniques have been applied to batch bioreactors, Sadhukhan et al.[5] varied nutrient concentrations important to the production of mycophenolic acid production. The yield of mycophenolic acid as a function of five nutrients were fit to a second-order polynomial equation. As more data were gathered, better estimates for the optimal nutrient concentrations were obtained.

A great deal of work on bioreactor control has been based only on simulation. Manchanda et al.[6] used this approach to compare neural-network techniques to proportional-integral (PI) and other advanced controllers. Chang and Chen[7] studied the effects of substrate inhibition. Optimization techniques have also been applied to find ideal operating conditions for complex batch bioreactor models. Torres et al.[8,9] applied a nonlinear optimization method, based on a stochastic multi-start search algorithm. Two alternative nonlinear models of the system were used in the optimization problem.

Optimization techniques have been applied to continuous bioreactor models. Tsoneva and Patariska[10] developed an optimal control algorithm for a continuous fermentation process. This algorithm involves a three-layer control

† Biotechnology Department, MS 2203 Idaho National Engineering & Environmental Laboratory, P.O. Box 1625, 2525 Fremont Ave., Idaho Falls, ID 83415-2203. Telephone: (208) 526-8786. Fax: (208) 526-0828. E-mail: dstoner@inel.gov.

(1) Halme, A.; Karim, N. Expert systems for biotechnology. In *Biotechnology 4*, 2nd ed.; Rehm, J. J., Reed, G., Eds.; VCH: New York, 1991; Chapter 19.
(2) Hitzmann, B.; Lubbert, A.; Shugerl, K. An expert system approach for the control of bioprocesses. 1. Knowledge representation and processing. *Biotechnol. Bioeng.* **1992**, *39*, 33−43.
(3) Kishimito, M.; Kitta, Y.; Takecuchi, S.; Nakajima, M.; Yoshida, T. Computer control of glutamic acid production based on fuzzy clusterization of culture phases. *J. Ferment. and Bioeng.* **1991**, *72*, 110−114.
(4) Oishi, K.; Tominaga, M.; Kawato, A.; Abe, Y.; Imayasu, S.; Nanba, A. Application of fuzzy control theory to the sake brewing process. *J. Ferment. and Bioeng.* **1991**, *72*, 115−121.
(5) Sadhukhan, A. K.; Murthy, M. R.; et al. Optimization of mycophenolic acid production in solid-state fermentation using response surface methodology. *J. Ind. Microbiol. Biotechnol.* **1999**, *22*, 33−38.
(6) Manchanda, S.; Willis, M. J.; et al. An appraisal of nonlinear control philosophies for application to a biochemical process. In *Proceedings of the 1991 IEEE American Control Conference*; Boston, 1991; p 1317.
(7) Chang, H.; Chen, L. Bifurcation characteristics of nonlinear systems under conventional PID control. *Chem. Eng. Sci.* **1984**, *39*, 1127−1142.
(8) Rodriguez-Acosta, F.; Regalado, C. M.; Torres, N. V. Nonlinear optimization of biotechnological processes by stochastic algorithms: Application to the maximization of the production rate of ethanol, gycerol and carbohydrates by *Saccharomyces cerevisiae*. *J. Biotechnol.* **1999**, *68*, 15−28.
(9) Torres, N. V.; Voit, E. O.; Gonzalez-Alcon, C. Optimization of nonlinear biotechnological processes with linear programming: application to citric acid production by *Aspergillus niger*. *Biotechnol. Bioeng.* **1996**, *94*, 247−258.
(10) Tsoneva, R. G.; Patarinska, T. D. Optimal control of continuous fermentation processes. *Bioprocess Eng.* **1995**, *32*, 189−196.

10.1021/op0100091 CCC: $20.00
Published on Web 05/18/2001

structure that takes a system from startup to optimal steady-state conditions in minimal time. The control structure relies on optimizing a mathematical model of the fermentation process by a decomposition method, based on an augmented Lagrange function. Nguang and Chen[11] also modeled a continuous fermentation process with a set of differential equations. Applying a recursive least-squares algorithm to the discretized model results in an online estimation scheme for optimal set points of feed concentration and dilution rates. This method is similar to Model Predictive Control.

Rational design and control of continuous, dynamic, and uncharacterized bioprocess is an extremely complex task; as the composition of the feed materials can vary with time, process parameters may vary, and many interacting species of microorganisms may be involved. Model-based optimization procedures require some understanding of the system to which they are being applied. Thus, they are inappropriate control technologies for the uncharacterized, highly variable bioprocesses. In addition, the changing physical and chemical conditions and microbial populations in dynamic bioprocesses make it vital that the control system be robust and able to adapt to changing conditions. Because learning-based control systems require a minimum of information before being implemented, they address the requirements for mining bioprocesses better than knowledge- or model-based control systems. Furthermore, the conventional approach to characterizing the effects of process parameters on microbial activity is to vary one parameter at a time, while holding all other conditions constant. Many of these experiments assume that parameter effects are de-coupled or independent of each other. Experiments that vary one parameter at a time provide a considerable amount of data. However, these types of experiments may not be appropriate for evaluating the metabolic response of microorganisms to a "real world" bioprocessing environment such as a mineral leaching or environmental remediation in which multiple parameters are continuously changing. A process optimization scheme that simultaneously varies more than one parameter is required to better understand the response of bacteria to the changing physical and chemical conditions that may be encountered within a mining environment. Therefore, the objective of this study was to evaluate the ability of the hybrid control system, with its integral "learning" program, to control and optimize a process for which little expert knowledge and no analytical model was available. Details of the microbiological response to changing conditions were previously presented elsewhere.[12]

2. Biological System Description

Two iron-oxidizing bacterial cultures that thrive in acidic environments were used in this study. The cultures differed in their carbon source requirements, their growth temperature range, and the amount of "expert knowledge" that was available. One culture was an uncharacterized moderate thermophilic culture that was obtained from a mining operation by cultivation at 55 °C in an acidic medium (pH 1.8) containing yeast extract and iron.[12] In contrast, the second iron-oxidizing culture, *Acidithiobacillus (Thiobacillus) ferrooxidans*, has been well characterized in over 50 years of study.[13] This bacterium uses carbon dioxide as its carbon substrate and grows well in acidic medium (pH $\approx$ 2) within a temperature range of 20−32 °C. There have been many studies that have examined the effects of parameters such as pH, temperature, air and CO_2 sparging rates, heavy metal concentration, and medium composition on the metabolism of *A. ferrooxidans*.[14−21] In addition, the bioenergetics and genetics involved with mineral oxidation have been examined in great detail,[22,23] and there have been a number of analytical models developed which are used to describe mineral oxidation by this bacterium.[24−27]

The majority of bioprocesses, particularly fermentation processes for the food, pharmaceutical, and specialty chemical industries, utilize pure cultures that have been well described. At the start of this study, the number of distinct species present in the enrichment culture was unknown.[12] Furthermore, all that was known about the culture was the cultivation medium, relative growth rate, and temperature range.[12] The metabolic mechanisms and yield coefficients for iron oxidation by the uncharacterized culture were unknown. Thus, there was insufficient information to develop a model for the enrichment culture.

(11) Nguang, S. K.; Chen, X. D. Recursive least squares scheme for operating a class of continuous fermentation processes at optimal steady-state productivity. *J. Chem. Technol. Biotechnol.* **1998**, *73*, pg. 227−232.

(12) Stoner, D. L.; Miller, K. S.; Fife, D. J.; Larsen, E. D.; Tolle, C. R.; Johnson, J. A. Use of an intelligent control system to evaluate multiparametric effects on iron oxidation by thermophilic bacterial. *Appl. Environ. Microbiol.* **1998**, *64*, 4555−4565.

(13) Vishniac, W.; Santer, M. The Thiobacilli. *Bact. Rev.* **1957**, *21*, 195−213.

(14) Hirose, T.; Suzuki, H.; Inagaki, K.; Tanaka, H.; Tano, T.; Sugio, T. Inhibition of sulfur use by sulfite ion by *Thiobacillus ferrooxidans*. *Agric. Biol. Chem.* **1991**, *55*, 2479−2484.

(15) Lazaroff, N. Sulfate requirement for iron oxidation by *Thiobacillus ferrooxidans*. *J. Bacteriol.* **1963**, *85*, 78−83.

(16) Mustin, C.; deDonato, P.; Berthelin, J.; Marion, P. Surface sulfur as promoting agent of pyrite leaching by *Thiobacillus ferrooxidans*. *FEMS Microbiol. Rev.* **1993**, *11*, 71−78.

(17) Nagpal, S.; Dahlstrom, D. Effect of carbon dioxide concentration on the bioleaching of a pyrite-arsenopyrite ore concentrate. *Biotechnol. Bioeng.* **1993**, *41*, 459−464.

(18) Pronk, J. T.; deBruyn, J. C.; Bos, P.; Kuenen, J. G. Anaerobic growth of *Thiobacillus ferrooxidans*. *Appl. Environ. Microbiol.* **1992**, *58*, 2227−2230.

(19) Suzuki, I.; Takeuchi, T. L.; Yuthasastrakosol, T. D.; Oh, J. K. Ferrous iron and sulfur oxidation and ferric iron reduction activities of *Thiobacillus ferrooxidans* are affected by growth on ferrous iron, sulfur or a sulfide ore. *Appl. Environ. Microbiol.* **1990**, *56*,1620−1626.

(20) Suzuki, I.; Lizama, H. M.; Tackaberry, P. D. Competitive inhibition of ferrous iron oxidation by *Thiobacillus ferrooxidans* by increasing concentration of cells. *Appl. Environ. Microbiol.* **1989**, *55*, 1117−1121.

(21) Tuttle, J. H.; Dugan, P. R. Inhibition of growth, iron, and sulfur oxidation by *Thiobacillus ferrooxidans* by simple organic compounds. *Can. J. Microbiol.* **1976**, *22*, 719−730.

(22) Pronk, J. T.; Liem, K.; Bos, P.; Kuenen, J. G. Energy transduction by anaerobic ferric iron respiration in *Thiobacillus ferrooxidans*. *Appl. Environ. Microbiol.* **1991**, *57*, 2063−2068.

(23) Rawlings, D. E., Kusano, T. Molecular genetics of *Thiobacillus ferrooxidans*. *Microbiol. Rev.* **1994**, *58*, 39−55.

(24) Gómez, J. M.; Caro, I.; Cantero, D. Kinetic equation for growth of *Thiobacillus ferrooxidans* in submerged culture over aqueous ferrous sulphate solutions. *J. Biotechnol.* **1996**, *48*, 147−152.

(25) Gómez, J. M.; Caro, I.; Cantero, D. Modeling of ferrous sulphate oxidation by *Thiobacillus ferrooxidans* in discontinuous culture: influence of temperature, pH and agitation rate. *J. Ferment. Bioeng.* **1996**, *86*, 79−83.

(26) Jones, C. A.; Kelly, D. P. Growth of *Thiobacillus ferrooxidans* on ferrous iron in chemostat culture: influence of product and substrate inhibition. *J. Chem. Technol. Biotechnol.* **1983**, *33B*, 241−261.

(27) Nemati, M.; Webb, C. A kinetic model for biological oxidation of ferrous iron by *Thiobacillus ferrooxidans*. *Biotechnol. Bioengineer.* **1997**, *53*, 478−486.

3. Control System Description

Once the continuous bioreactor was inoculated with the cultures discussed above, the optimal operating conditions of the bioreactor needed to be determined. The conditions important for maximum bioreactor production include:

- inlet volumetric flow
- inlet iron(II) concentration
- pH of the chemostat
- temperature of the chemostat

These variables are relevant to a mineral leaching process. Inlet iron concentration pertains to the process at hand, that is, the production of oxidized iron. Temperature and pH are physicochemical parameters that can significantly impact the growth and activity of microorganisms and are usually control variables in biological processes. Other parameters which were measured, for example, oxygen concentration, dissolved CO_2, redox potential, were not selected as variables for evaluating the stochastic learning algorithm because there were no appropriate methods for controlling these parameters within our system. The computer was used to control nutrient feeds, pH using acid and base pumps, gas-flow valves, a heater, and a stirrer.[12] Gas flow rates were regulated via the gas mass flow controllers but were not integrated into any feedback control loops. The feed rate and inlet nutrient and iron concentrations were delivered as specified using an integrated set of pumps with fuzzy controllers. The pump controllers automatically re-calibrated to ensure accurate dilution rates and feed concentrations. Liquid level (working volume ~1360 mL) was maintained by a drain tube located on the side of the chemostat.

An on-line sensor system measured temperature (Cole-Parmer, Vernon Hills, IL), pH (Ingold Electrodes, Inc., Wilmington, MA), oxidation−reduction potential (Ingold Electrodes, Inc., Wilmington, MA), and dissolved oxygen concentration (Ingold Electrodes, Inc., Wilmington, MA). Off-line measurements were made for biomass as determined by direct cell counts, iron(II) concentration, iron(III) concentration, total organic carbon (TOC) and dissolved organic carbon (DOC). For cell counts, cells were collected by filtration, stained on the filter with acridine orange (total counts) or fluorescein-conjugated wheat germ agglutinin for the Newmont thermophilic culture, and viewed using epifluorescence microscopy.[28] The concentration of iron(II) in duplicate samples was determined by titration with potassium dichromate or potassium permanganate.[29] The concentration of iron(III) in filtered samples was determined in duplicate by ultraviolet absorption spectroscopy at a wavelength of 304 nm.[30] Total iron was calculated by summation of the average of the iron(II) and iron(III) concentrations. TOC and DOC were determined on unfiltered and filtered samples, respectively, using a Shimadzu model TOC 5000 total organic carbon analyzer.

Optimality was determined by defining productivity as follows:

$$P = f\,(P_{\mathrm{IRON}}) + (1 - f)(P_{\mathrm{CELLS}}) \tag{1}$$

Where:

$$0 \le f \le 1 \tag{2}$$

$$P_{\mathrm{IRON}} = \left[\frac{[\mathrm{Fe}^{+3}]}{[\mathrm{Fe}^{+2}] + [\mathrm{Fe}^{+3}]}\right] \times F_{\mathrm{rate}}^{\mathrm{current}} \tag{3}$$

$$P_{\mathrm{CELLS}} = \left[\frac{\text{suspended cell numbers}}{1 \times 10^{8}}\right] \times F_{\mathrm{rate}}^{\mathrm{current}} \tag{4}$$

The resulting optimization problem then becomes to find the flow rate (F), inlet iron(II) concentration ($[\mathrm{Fe}^{2+}]$), pH of chemostat (pH), and temperature of chemostat (T) that result in a maximum productivity. In this paper, productivity was defined as being dependent only on the conversion of iron(II) to iron(III). Thus, $f = 1$ and only iron(II) concentration, iron(III) concentration, and the flow rate need to be measured to calculate productivity. This section describes a supervisory control system, the BioExpert, and two of its sub-controllers; the flow-rate controller and the stochastic optimization procedure that are designed to solve this optimization problem.

The stochastic optimization algorithm and flow controller interact as follows:

1. Set the algorithm step counter, k, to 0. Run the reactor to steady state for a given temperature ($SetPt_{\mathrm{current}}^{\mathrm{temperature}}$), pH ($SetPt_{\mathrm{current}}^{\mathrm{pH}}$), iron(II) concentration ($SetPt_{\mathrm{current}}^{\mathrm{Fe}}$), and flow rate ($F_{\mathrm{rate}}^{\mathrm{current}}$) combination.
2. Calculate the production rate, P_k, (see eqs 1−4).
3. Pick a new flow rate based on algorithm defined in Section 3.1, $F_{\mathrm{rate}}^{\mathrm{current}}$, $k = k + 1$.
4. Run the reactor to steady state (see steady-state criterion below).
5. Calculate the production rate, P_k, (see eqs 1−4).
6. Has the peak production rate, P_k, for this set point step (temperature, pH, and iron concentration) been reached?

   If $k \ge 4$ and $|P_k - P_{k-1}| \le 1$ mL, then

   YES: pick a new pH, temperature, and iron(II) concentration based on the stochastic learning algorithm defined in section 3.2

   go to Step 1

   Else

   NO: go to Step 3

Determining whether the chemostat is operating at steady-state was one of the key steps used by the BioExpert. Using the on-line and off-line data and messages concerning changes in set points, the BioExpert determined whether the chemostat was in transition, at steady state or being "washed out". Reactor-state determinations were made using the following criteria. The reactor was defined to be at steady

(28) Fife, D. J.; Bruhn, D. F.; Miller, K. S.; Stoner, D. L. Evaluation of a Fluorescent Lectin-Based Staining Technique for some Acidophilic Mining Bacteria. *Appl. Environ. Microbiol.* **2000**, *66*, 2208−2210.

(29) Skoog, D. A.; West, D. M. Applications of strong oxidizing agents. In *Fundamentals of Analytical Chemistry*, 2nd ed.; Holt, Rinehart and Winston, Inc.: New York, 1969; Chapter 19, pp 418−444.

(30) Steiner, M.; Lazaroff, N. Direct method for continuous determination of iron oxidation by autotrophic bacteria. *Appl. Microbiol.* **1974**, *28*, 872−880.

state when the following conditions were met:

- no set point changes for at least 5 residence times
- the redox values change less than 10%
- the [Fe^{2+}] and [Fe^{3+}] concentrations change less than 10%
- TOC changes less than 25%

Likewise, the reactor was defined to be at washout when all of the following conditions were met:

- more than two residence times had passed since last set point change
- TOC decreased by more than 50%
- redox values decreased by more than 25%
- [Fe^{2+}] concentration increased by more than 10%
- [Fe^{3+}] concentration decreased by more than 10%

If the reactor was not at steady state or at washout, it was said to be in transition. This occurred whenever a set point was changed and the conditions for the other two states had not been met.

3.1. Best Fit Control of Flow. The flow-rate controller discussed above was based on the combination of an expert system and a best-fit control concept. This controller was used to "fine-tune" the flow rate for each set of environmental conditions set by the stochastic learning algorithm. When environmental conditions remain constant (i.e., temperature, inlet iron(II) concentration, and pH), the productivity increases with increasing flow rate (see eqs 1−4). However, increasing the flow rate also decreases the residence time in the chemostat and promotes washout conditions. Due to these off-setting dynamics, the best-fit control concept assumed that flow rate, F_{rate}, versus productivity, P, fits a parabolic curve for a fixed set of environmental conditions. On the basis of expert knowledge, the flow-rate control system selected the initial three flow rates for the best-fit control algorithm, see below. Using the productivity values from the three initial flow rates, the best-fit controller solved for the flow rate that maximizes the parabolic productivity curve. Additional flow-rate data were added to the initial data for each new iteration.

The flow rate expert system was defined as follows:

1. The initial flow rate, F^1_{rate} was selected by the operator for the first controller parameter set including pH, temperature, and inlet iron(II) concentration. Alternatively, the expert system initializes its flow rate using the center of the allowable range, in this case 5 mL/min. For the subsequent control parameter sets, the first flow rate evaluated in each set of parameters was the last flow rate evaluated in the previous set ($SetPt^{temperature}_{current}$, $SetPt^{pH}_{current}$, $SetPt^{Fe}_{current}$). For example, the first flow rate evaluated in Run D, was the last flow rate evaluated in Run C.

2. The second flow rate was chosen using the following logic:

$$\text{If} \quad F^1_{rate} \leq 7\,\frac{mL}{min} \quad \text{then}$$

$$F^{target}_{rate} = 1.5F^1_{rate}$$

Else

$$F^{target}_{rate} = \frac{F^1_{rate}}{1.5}$$

3. The third flow rate was chosen as:

If $F^1_{rate} \leq F^2_{rate}$ then

$$\text{If} \quad P(F^1_{rate}) \leq P(F^2_{rate}) \quad \text{then}$$

$$F^{target}_{rate} = 1.5F^2_{rate}$$

Else

$$F^{target}_{rate} = \frac{F^1_{rate}}{1.5}$$

Else

$$\text{If} \quad P(F^2_{rate}) \leq P(F^1_{rate}) \quad \text{then}$$

$$F^{target}_{rate} = 1.5F^1_{rate}$$

Else

$$F^{target}_{rate} = \frac{F^2_{rate}}{1.5}$$

4. After three flow rates had been evaluated, the flow controller switched from the expert system to the parabolic fitting algorithm. A least squares parabolic fit for productivity, P, versus flow rate, F_{rate}, curve was obtained by solving the following equation:

$$AB = Y \tag{5}$$

where

$$A = \begin{bmatrix} 1 & F^1_{rate} & (F^1_{rate})^2 \\ 1 & F^2_{rate} & (F^2_{rate})^2 \\ & \cdot & \\ & \cdot & \\ & \cdot & \\ 1 & F^{current}_{rate} & (F^{current}_{rate})^2 \end{bmatrix} \tag{6}$$

$$B = [b_0\ b_1\ b_2]^T \tag{7}$$

Equation 5 was solved using a singular value decomposition

$$Y = [P(F^1_{rate})\ P(F^2_{rate}) \ldots P(F^{current}_{rate})]^T \tag{8}$$

(SVD) that produced the pseudo-inverse of A on the left. After a parabolic fit to the data was obtained, the critical point of the parabola was used to calculate the next flow rate target.

$$P_{target} = P(F^{target}_{rate}) = b_0 + b_1F^{target}_{rate} + b_2(F^{target}_{rate})^2 \tag{9}$$

$$\frac{dP(F^{target}_{rate})}{dF^{target}_{rate}} = b_1 + 2b_2F^{target}_{rate} = 0 \tag{10}$$

$$F^{target}_{rate} = \frac{-b_1}{2b_2} \tag{11}$$

5. For the subsequent flow rates, the parabolic fitting algorithm from the previous step was repeated.

3.2. Stochastic Learning Controllers. A stochastic learning algorithm[31] was used to determine the optimal pH,

(31) Johnson, J. A.; Stoner, D. L.; Larsen, E. D.; Miller, K. S.; Tolle, C. R. Learning-Based Controller for Biotechnology Processing, and Method of Using. U.S. Pat. Appl., Docket No. 14233.12.

temperature, and iron concentration set points. This algorithm was similar to, but distinct from, one investigated by Moore[32] and Franklin.[33] Instead of a traditional Gaussian density function, the density function consisted of two-half-Gaussian density functions. The approach differed in that the learning algorithm unevenly biased the two-sided Gaussian density functions that were used to choose the next set point. This was done to bracket the optimal solution more readily.

By using the mean of two-half-Gaussian density functions, which are divided at each one's traditional mean, the mean of this new density function remains the same as a traditional Gaussian.

$$\bar{x} = \int_{-\infty}^{+\infty} x\, f_x(x)\mathrm{d}x \tag{12}$$

$$= \frac{1}{\sqrt{2\pi\sigma_L^2}} \int_{-\infty}^{\hat{m}} x \exp\left(\frac{-(x-\hat{m})^2}{2\sigma_L^2}\right) \mathrm{d}x + \frac{1}{\sqrt{2\pi\sigma_R^2}} \int_{\hat{m}}^{+\infty} x \exp\left(\frac{-(x-\hat{m})^2}{2\sigma_R^2}\right) \mathrm{d}x \tag{13}$$

$$= \frac{\hat{m}}{2} + \frac{\hat{m}}{2} \tag{14}$$

$$= \hat{m} \tag{15}$$

The learning algorithm operated simultaneously for the three parameters that were evaluated, pH ($SetPt_x^{\mathrm{pH}}$), temperature ($SetPt_x^{\mathrm{temperature}}$), and iron concentration ($SetPt_x^{\mathrm{Fe}}$). The initial mean was chosen as a guess at where the productivity, P, maximum was located (Figure 1a, Table 1). The initial widths or standard deviations (σ_R^x and σ_L^x) of the density functions were chosen to span a reasonable operating range for each parameter (Figure 1a, Table 1).

The stochastic learning takes place by adjusting the density functions, that is, mean and standard deviation, depending on the relative production rates. If the production rate improved with a tested set point, T_1, the new mean ($\hat{m}$) of the density function was shifted to that set point. Also, the right and left standard deviations were changed to reflect the shift of the density function towards the increase in productivity (Figure 1b). For example, if an increase in temperature resulted in an increase in productivity, the right side standard deviation was increased and the left side standard deviation was decreased. However, if the rate did not improve, the mean of the density function did not change, and the width of the density function in the direction of the set point was decreased, and the other side's width was increased (Figure 1c). The choice for each new set point was made by using a random number generator based on the new two-sided Gaussian density functions (such as T_1 in Figure 1a).

The current stochastic learning algorithm is summarized as follows:

Initialize the density functions:

$$SetPt_{\mathrm{best}}^x = \hat{m}^{\bar{x}}$$

$$\sigma_R^x = \sigma_{iR}^x$$

$$\sigma_L^x = \sigma_{iL}^x$$

Repeat forever:

Select $SetPt_{\mathrm{current}}^x$, evaluate P_{current}

Calculate the standard deviation change:

$$\Delta\sigma^x = Sc^x \left| \frac{SetPt_{\mathrm{current}}^x - SetPt_{\mathrm{best}}^x}{SetPt_{\mathrm{best}}^x} \right|$$

If $P_{\mathrm{current}} > P_{\mathrm{best}}$

If $SetPt_{\mathrm{best}}^x < SetPt_{\mathrm{current}}^x$ then

$SetPt_{\mathrm{best}}^x = SetPt_{\mathrm{current}}^x$

$P_{\mathrm{best}} = P_{\mathrm{current}}$

$\hat{m}^{\bar{x}} = SetPt_{\mathrm{current}}^x$

$\sigma_R^x = \sigma_R^x + \Delta\sigma^x$ and

$\sigma_L^x = \sigma_L^x - \Delta\sigma^x$

Else

$SetPt_{\mathrm{best}}^x = SetPt_{\mathrm{current}}^x$

$P_{\mathrm{best}} = P_{\mathrm{current}}$

$\hat{m}^{\bar{x}} = SetPt_{\mathrm{current}}^x$

$\sigma_R^x = \sigma_R^x - \Delta\sigma^x$ and

$\sigma_L^x = \sigma_L^x + \Delta\sigma^x$

Else

If $SetPt_{\mathrm{best}}^x < SetPt_{\mathrm{current}}^x$ then

$\sigma_R^x = \sigma_R^x - \Delta\sigma^x$ and

$\sigma_L^x = \sigma_L^x + \Delta\sigma^x$

Else

$\sigma_R^x = \sigma_R^x + \Delta\sigma^x$ and

$\sigma_L^x = \sigma_L^x - \Delta\sigma^x$

If $\sigma_R^x < 0.001$ then $\sigma_R^x = 0.001$

If $\sigma_L^x < 0.001$ then $\sigma_L^x = 0.001$

Loop

Please note that x represents either pH, temperature, or inlet iron(II) concentration (see Tables 1 and 2 for initial values and scaling factors).

4. Results of Flow-Rate Control

The effect of the flow rate controller was initially investigated. The data gathered from this investigation is

(32) Moore, K. L. *Iterative learning control for deterministic systems*; Series on Advances in Industrial Control; Springer-Verlag: New York, 1993.

(33) Franklin, J. A. Refinement of robot motor skills through reinforcement learning. *Proceedings of the IEEE 27th International Symposium on Decision and Control*; IEEE Control Systems Society; New York, NY, pp 1096−1101.

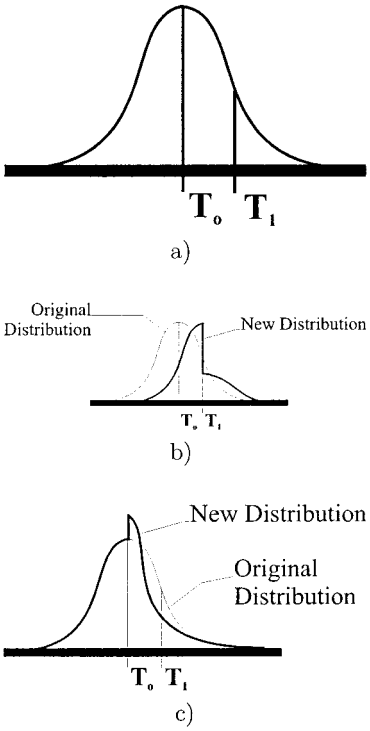

Figure 1. **Two-sided Gaussian: (a) initial density function, (b) improvement in productivity, and (c) no improvement in productivity.**

Table 1. **Initial Gaussian density functions ($\bar{x}$, σ_R^x, σ_L^x)**

x	$\hat{m}^{\bar{x}}$	σ_R^x	σ_L^x
pH	1.8	0.5	0.5
temperature	45	5.0	5.0
$[Fe^{2+}]$	50	15.0	15.0

Table 2. **Scaling factors for $\Delta\sigma^x$ calculations**

x	Sc^x
pH	0.17
temperature	1.67
$[Fe^{2+}]$	5.0

shown in Table 3. The stochastic learning controller set the operating environments and the flow controller selected a sequence of flow rates attempting to produce the optimal productivity for each set of operating parameters. The values reported for suspended cell density, $[Fe^{3+}]$, conversion, and production (mL/min) are the values obtained when the chemostat was operated at the flow rate that achieved the maximum iron production for that set of conditions. Figure 2 (Run F) shows a typical parabolic fitting to estimate optimum flow rate.

For Run A (pH 1.8, 45 °C, 50 mM $[Fe^{2+}]$) productivity data for flow rates of 4, 6, and 9 mL/min were fitted to a parabola and used predict optimum productivity at a flow of 7.01 mL/min. This flow rate was validated by the final run at a flow rate of 7 mL/min.

There was no curve fitting procedure for Run B (pH 1.84, 51.5 °C, 47.15 mM $[Fe^{2+}]$) which was terminated by the operator due to washout even at the lower flow rate of 2.0 mL/min. Run C (pH 1.8, 45 °C, and 50 mM iron) was a repeat of run A to assess whether the chemostat had *recovered* from near washout conditions. A comparison of data obtained from runs A and C indicates that the microorganisms recovered from an adverse environment.

During Run D, the computer had predicted that maximum productivity would occur at 11.2 mL/min. The final productivity for this run was a value of 5.183 mL/min compared to 8.5 mL/min that was achieved at a flow rate of 11.1 mL/min. Nevertheless, because the final curve fitting procedure using the complete set of data had a optimal flow rate that was comparable to the one that was predicted (11.2 mL/min), the data set was considered validated, and the computer selected the next set of parameters to evaluate.

Run E was not completed due to a malfunction in the hard drive the computer. During Run F (see Figure 2), six flow rates were required to select and validate the maximum productivity. A rather shallow curve was obtained that did not have a strong maximum. Comparable productivity values were obtained at the similar flow rates that were evaluated in both Runs E and F.

Run G (see Figure 3; pH 2.3, 39.7 °C, and 45.5 mM iron) illustrated a situation where the range of achievable flow rates did not contain the global optimum. The productivity was so low that it could only be improved by increasing flow rate. Since the initial values were only on one side of the parabola, the curve fitting procedure produced in an inverted parabola and a target maximum could not be determined. Human operators ultimately terminated the run because requested flow rates had exceeded the pumping capacity of the small tubing that was installed in the peristaltic pumps. If the higher flow rates could have been achieved, the washout dynamics would have been more significant and on optimum flow rate should have been found. Nevertheless, for purposes of discussion and comparison to other runs, the data obtained at the flow rate of 12.75 was utilized.

The behavior of the reactor in Run H (pH 1.7, 39.9 °C, and 39.9 mM iron) was such that the maximum productivity was easily predicted and validated according to the programmed procedure.

5. Results of Learning-Based Control

Now we examine the results of the stochastic learning controller. To set the initial conditions and scaling factors, some knowledge of the culture is required. However, little was known about this iron-oxidizing culture other than it was "enriched" from a sample acquired from a heap leaching operation by cultivation at 55 °C in an acidic (pH 1.8) medium containing yeast extract and Fe^{2+}.[34] With this vague knowledge, runs 1−6 in Table 4 were operated with the control decisions made by the human operator using the conventional approach of varying a single parameter while holding the others constant. This portion of the experiment was run at a pH 2, an inlet iron(II) concentration of 50 mM and a flow rate of 7mL/min with temperatures of 40, 30, 50, 45, and 60 °C (see Table 4). Steady-state control

(34) Brierley, J. A. Personal communication, 1996.

Table 3. **Effects of multi-parametric changes on the growth and iron oxidation by the Newmont moderately thermophilic culture**

	parameter Set				values at maximum productivity			
run	°C	pH	inlet [Fe^{2+}] (mM)	flow rates (mL/min)	biomass (cells/mL)	outlet [Fe^{3+}] (mM)	conversion (%)	productivity (mL/min)
A	45	1.8	50	4, 6, 9, 7.03[a]	7.6×10^7	45.08	86.6	6.31
B	51.5	1.84	47.15	7,2[a]	2.91×10^5	4.24	9.6	0.19
C	45	1.8	50	7, 4.67, 10.5, 7.45[a]	7.33×10^7	42.88	83.1	6.193
D	40.7	1.9	34.48	7.45, 4.93, 11.1, 12, 11.2[a]	1.62×10^7	16.28	46.3	5.183
E	53.3	1.64	60.65	11.1, 7.4, 12, 9.6[a]	incomplete run - no data			
F	53.3	1.64	60.65	4. 5, 7.5, 11.25, 9.17, 12, 8.52[a]	2.98×10^7	35.56	57.4	4.891
G	39.7	2.3	45.5	8.55, 5.73, 12, 12.75[b], 15.4, 21	2.28×10^7	5.4	11.3	1.4
H	39.9	1.7	39.94	5.2, 7.8, 11.7, 9.19[a]	3.14×10^7	27.74	68.3	6.32

[a] Values obtained at the flow rate for which maximum productivity was achieved. [b] Liquid feed system unable to deliver calculated flow rate. Values are for flow rate of 12.75 mL/min.

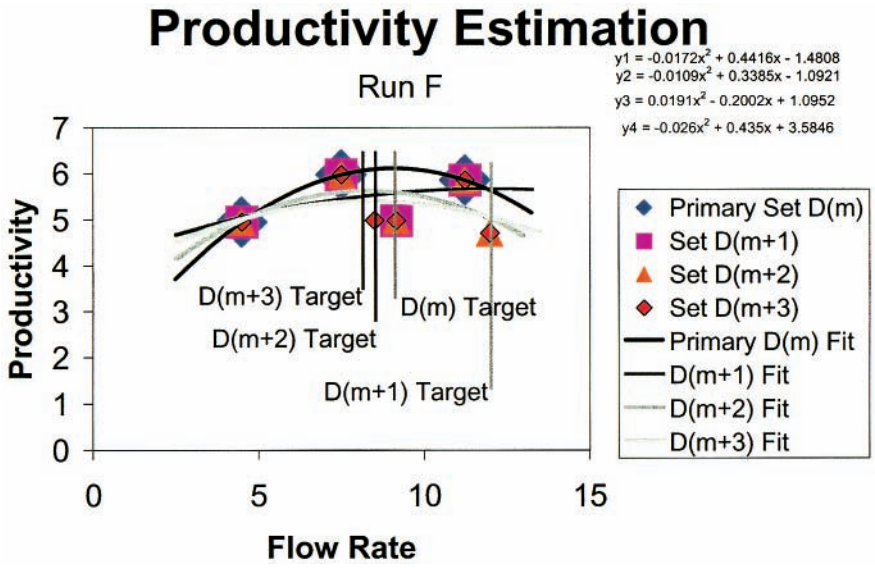

Figure 2. **Run F flow-rate calculations.**

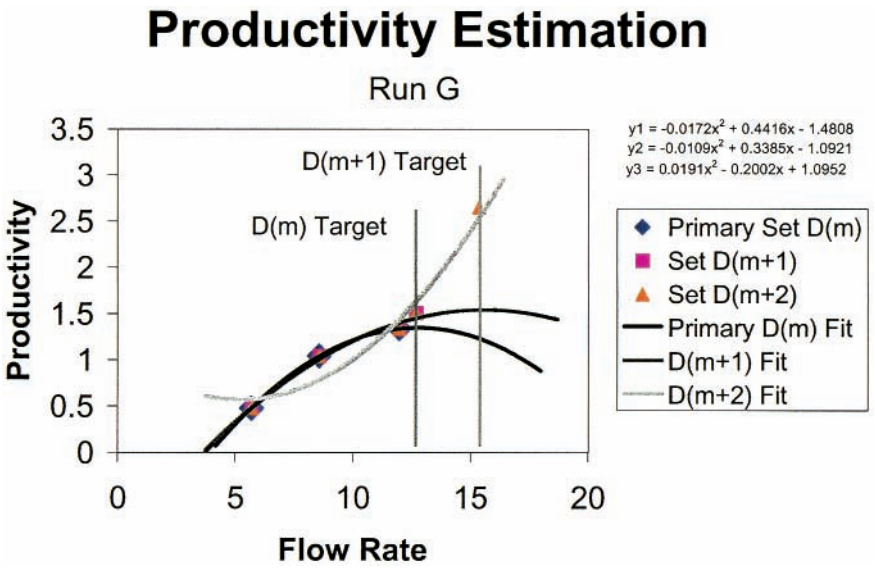

Figure 3. **Run G flow-rate calculations.**

descisions were made with an intelligent control system described by Stoner at al.[12] The productivity during these runs was moderate and the reactor was not in danger of a "washout" situation and a valid starting point was established.

With knowledge about an acceptable temperature range and valid initial conditions, the stochastic learning controller and flow controller was operated. Data from these runs when the flow rate was near 7mL/min are shown as runs 7−15 in

Table 4. **Effects of multiparametric changes on the growth and iron oxidation by the Newmont moderately thermophilic culture (near constant flow rate)**

	parameter Set				values at maximum productivity			
run	°C	pH	inlet [Fe^{2+}] (mM)	flow rates (mL/min)	biomass (cells/mL) × 10^{-6}	outlet [Fe^{3+}] (mM)	conversion (%)	productivity (mL/min)
1	40	2	50	7	9.9	21.96	42.9	3.005
2	30	2	50	7	4.71	19.66	37.8	2.647
3	50	2	50	7	18.7	23.64	47.1	3.294
4	45	2	50	7	14.2	19.94	39.1	2.740
5	55	2	50	7	21.2	20.74	41.0	2.873
6	60	2	50	7	1.7	12.22	24.2	1.697
7	45	1.8	50	7.03	76	45.08	86.6	6.091
8	45	1.8	50	7	105	48.8	95.6	6.711
9	51.5	1.84	47.15	7	4.4	10.27	21.4	1.497
10	45	1.8	50	7	82.9	43.12	83.7	5.859
11	45	1.8	50	7.45	73.3	42.88	83.1	6.193
12	40.7	1.9	34.48	7.4	29	27.7	81.8	6.064
13	53.3	1.64	60.65	7.4	85.1	46.36	76.5	5.660
14	53.3	1.64	60.65	7.5	70.4	48.32	76.0	5.701
15	39.9	1.7	39.94	7.8	31.5	26.92	65.2	5.084
16	32	1.7	50	7	35.8	22.04	43.2	3.023
17	38.7	1.69	17.14	7	21.3	0.769	4.3	0.303
18	34	1.69	53.61	7	1.0	2.45	4.5	0.315
19	45	1.87	51.33	7	66.5	32.28	63.1	4.417
20	43	1.94	16.82	7	54.7	14.19	88.7	6.212
21	36.8	1.84	31.05	7	23	16.14	51.0	3.571
22	45.9	1.87	21.74	7	83.8	20.66	93.8	6.563
23	43.6	1.8	28.9	7	45.9	27.04	94.7	6.626
24	44	1.81	34	7	44.8	34.2	96.0	6.720

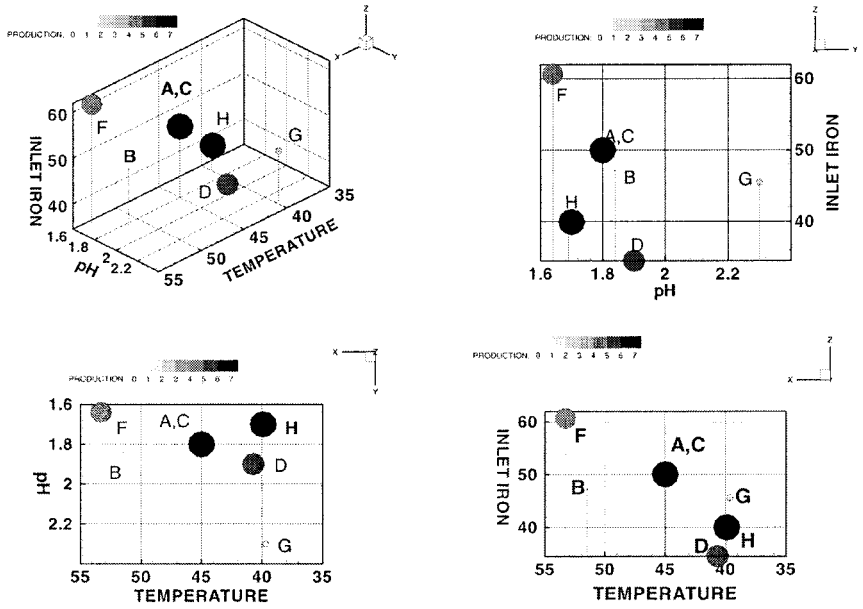

Figure 4. **The stochastic and flow optimization controllers four-dimensional learned productivity space.**

Table 4. The productivity during these runs was significantly higher than the first set of runs. This indicates that the stochastic learning algorithm should find the optimal operating conditions faster than the conventional technique. During runs 16−24 (see Table 4), the flow controller was not used and the flow rate was held constant at 7 mL/min. With this change, steady state conditions could be reached much faster and the stochastic learning controller performance could be evaluated independently from the flow controller.

The results shown in Figure 4 for the combined stochastic and flow rate optimization control system clearly show that the assumption of coupled environmental parameters is correct. This is an important result, since the biological community tends to assume the decoupling of the environmental parameters as they investigate a new bacterium. The productivity space for the entire series of runs is shown in Figure 5. By the end of the runs, the stochastic learning controller is consistently choosing operating conditions that result in over 90% iron(II) conversion. Please note that increased productivity corresponds to increased sphere diameter in Figures 4 and 5.

To contrast results obtained with the stochastic controller with alternative approaches we need to consider the data from the earlier experiment that are included in Figure 5 as runs

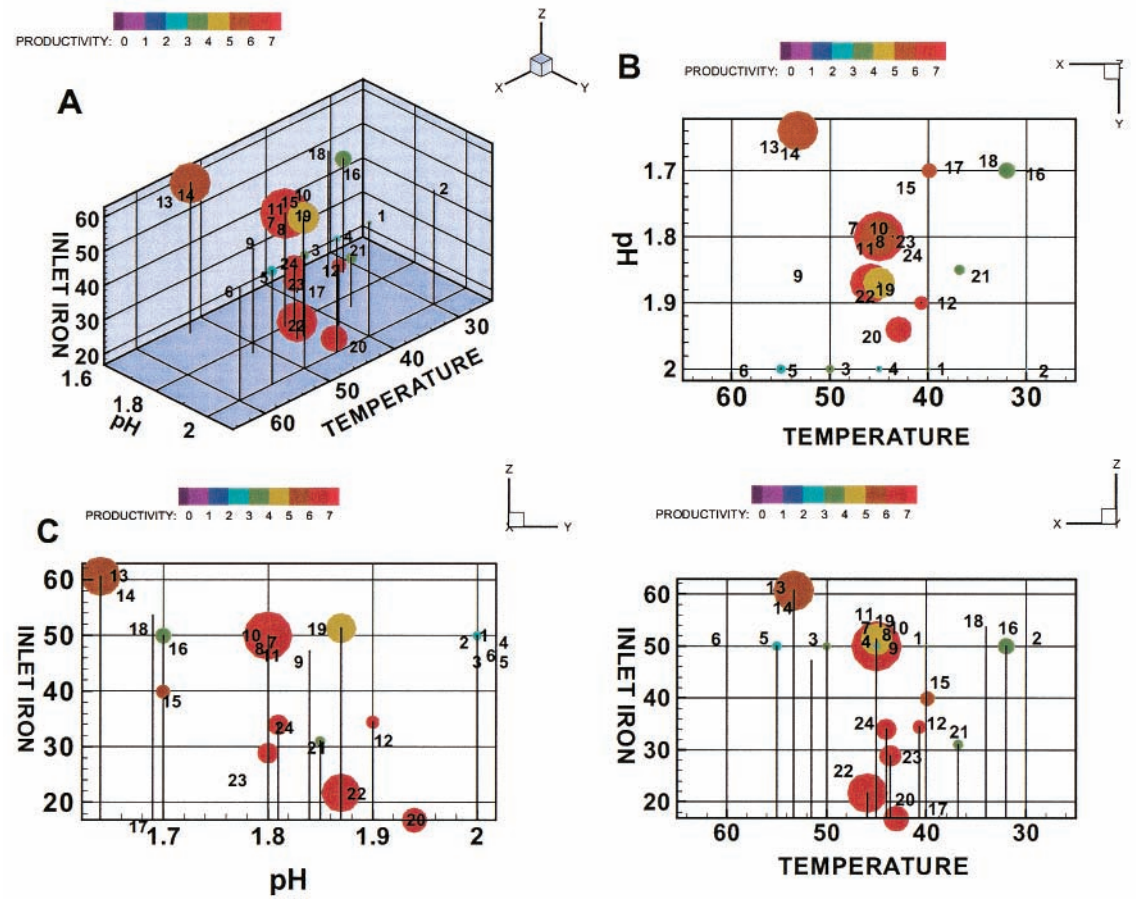

Figure 5. **The stochastic optimization controller four-dimensional learned productivity space.**

1−6. The results of this experiment had indicated that there was little effect of temperature on the productivity rate. This earlier conclusion that was dramatically different than the one reached later when pH, temperature, along with inlet iron concentration were varied and the interactive effects between pH and temperature could be discerned.

6. Conclusions

The standard assumption made in biological experimentation is that the *biological* controls, that is, the environmental parameters, are decoupled. This assumption allows for the search of an optimal production environment through the mapping of the data space one parameter at a time. This control system was designed around the opposite assumption, primarily that the biological controls are coupled. Through the testing of this system, it has been shown that coupled parameters is the only plausible assumption that can be made for this biological system.[12]

The current implementation of this system appeared to function as desired. Moreover, this reactor and control system provided a valuable *real world* means for testing new and improved control system concepts in model less environments. This not withstanding, many of the subsystems can be improved. Currently, this control system environment is being updated to test gas-phase limited substrates through permeable membranes. Methods for adding gradient based productivity updates are being studied as possible additions to the stochastic learning algorithm presented within this paper. Last, stochastic control techniques that do not require expert knowledge may be applied to the flow rate subcontroller. This control system serves as an example of what the microbiological research teams currently need for studying newly discovered uncharacterized microorganisms.

Acknowledgment

This work was supported by the Department of Energy, Office of Science, Basic Energy Sciences under DOE Idaho Operations Office Contract DE-AC07-99ID13727. We acknowledge Eric Larsen and Karen Miller for technical assistance.

Received for review January 29, 2001.

OP0100091